AIMS Materials Science, 11(2): 231–242.
DOI: 10.3934/matersci.2024013
Received: 21 November 2023
Revised: 12 January 2024
Accepted: 24 January 2024
Published: 21 February 2024

http://www.aimspress.com/journal/Materials

Research article

Recycling glass fiber-reinforced plastic in asphalt concrete production

Aleksei V. Shiverskii, Aleksandr V. Kukharskii, Stepan V. Lomov and Sergey G. Abaimov*

Center for Petroleum Science and Engineering, Skolkovo Institute of Science and Technology, Bolshoy Boulevard 30, bld. 1, Moscow, Russia

* **Correspondence:** Email: s.abaimov@skoltech.ru.

Abstract: Glass fiber-reinforced plastics (GFRP) have been produced in large quantities for over half a century and nowadays their waste has become a problem worldwide. Their recycling is difficult because they are predominantly manufactured from thermosetting matrices that are not suitable for secondary processing. Only few technologies are able to target full-scale utilization of residual mechanical performance at recycling, with the replacement of gravel in asphalt concrete being one of them. The possibility of introducing crushed GFRP (GFRP crumb) into asphalt concrete and its impact on mechanical characteristics have been investigated in our study. As the source of GFRP, road noise-protection fence was chosen due to large quantities of its waste accumulated in urban economy. Several approaches to produce crumbs were attempted with only shredding being successful. The GFRP crumb has provided excellent mechanical performance of asphalt concrete fabricated by standard routine. In particular, the improvement in compressive modulus was 40%, even under conditions of elevated asphalt concrete temperature at 50 °C. Besides, introduction of GFRP crumb reduced the overall weight of asphalt concrete mixture, providing further reduction of a carbon footprint. The results obtained indicated that recycling of GFRP waste as replacement of gravel in asphalt concrete provides an economically and environmentally safe solution.

Keywords: asphalt concrete; glass fibre-reinforced polymer; recycling

1. Introduction

Glass fiber-reinforced plastic (GFRP) is a composite material composed typically of an epoxy or other thermoset matrix reinforced by fine glass fibers. It is commonly employed in a wide range of

applications, from automotive parts to boat hulls and aircraft components [1]. Urban infrastructure and machinery also relies on large quantities of GFRP production. The annual global amount of GFRP products is approximately 8 million tons [2] and growing from year to year, with the expectation to double in the next 10–20 years [3]. The most widespread example of the application of GFRP in civil construction is the production of wind turbine blades [4].

Both production and disposal of GFRP can have negative environmental impacts, leading to the need for effective recycling and reprocessing methods [5]. Approximately 1.5 million tons of GFRP waste is produced annually [6], and there is a large accumulation of waste. With the example of wind turbine blades, one can see that the burial being the main method of GFRP recycling [4,7]. Although GFRP is not toxic, its burial leads to an increase in landfill areas, which does not meet the sustainable development of technology. Incineration is ecologically costly and does not put to use high residual mechanical performance, which disposed GFRP possesses. Active research is being conducted for the development of alternative methods for GFRP recycling [8,9]. Three major directions have been identified: mechanical [10], thermal [11,12], and chemical [13,14] processing. Chemical and thermal processing allows for the production of glass fiber as the end product, suitable for reuse in GFRP production [15], concrete reinforcement [16], and bitumen reinforcement [17]. Mechanical processing is the least labor-intensive, with the end product being GFRP crumb. GFRP crumb retains all residual GFRP properties, and its recycling technology is expected to aim mainly at providing good interface (adhesion) for load transfer. One such application could be as a reinforcing filler in civil engineering. GFRP crumb is actively discussed as an additive to concrete [18–20], but has been little studied as an additive to asphalt concrete production [21]. Partial replacement of gravel with the GFRP crumb (the so-called dry process [9]) will help to complete the GFRP recycling cycle while bitumen or another binder are expected to perform the role of the matrix for the GFRP crumb with the same ease as for mineral aggregates.

Adding some percent of GFRP in the pavement can cause health problems when it is being dismantled, as glass fibers present health hazards [22,23]. The problem is aggravated by the fact that glass fibers are degraded only under acidic or alkaline conditions, hence survive for indefinite time. Similar problems are being investigated in shipbuilding industry, where recycled materials contain large amount of GFRP [24]. In the construction industry, the problem is being studied in detail in relation to recycling of structures containing mineral wool, including glass wool [25].

We examined the effect of introduction of GFRP crumb into asphalt concrete on its strength properties. The scrap from GFRP road noise-protection fences was chosen to fabricate crumb. Noise-protection fences are widely applied in road construction and significant amount of their waste awaits recycling after the end of their service life.

2. Materials and methods

Due to the harmfulness of fiberglass dust for respiratory organs and human body [22,23], crushing of GFRP into crumbs is a separate, labor-intensive task. The employed SWP-800 shredder (Kooen Machinery, China) had a sealed system for removing crushed material, which provides safe working conditions for the operator. The scrap from the road noise-protection fence PHS (Flotenk, Russia) was used as raw material to produce GFRP crumb. Before crushing, the scrap was cut by circular saw into pieces no larger than 1 and 0.2 m in length and width, respectively, and the thickness of the PHS walls

was 3–8 mm. At 480 revolutions per minute of blades in the shredder, the scrap was crushed into GFRP crumb with fraction 0–20 mm. The crushing time for 100 kg of GFRP scrap was 20 min.

Asphalt concrete mixtures were prepared with road bitumen BND (Rosneft, Russia). As coarse and fine aggregates, granite crushed stones were used, as well as granite powder and sand (NerudStroi-M, Russia). GFRP crumb, granite crushed stones, granite powder, and sand were sifted through sieves by vibrating platform SMJ-538 (I-mach, Russia). Technical properties of materials shown in Table 1.

Table 1. Technical properties of materials.

Material	Characteristics	Sieve size, mm	In pure asphalt concrete mixture (wt.%)	In modified asphalt concrete mixture (wt.%)
Granite crushed stones	By GOST 8267-93, Grade M-1400	15	35	35
		10	15	14
		7.5	10	10
		5	15	14
		3	15	15
Sand	By GOST 8736-2014, Grade M-800	0.63	15	15
Granite powder	By GOST 16557–2005, Grade MP-1	0.315	5	5
Bitumen	By GOST 22245, Grade BND 60/90		5	5
GFRP crumb	Length:10–15 mm; Diameter: 0.315–0.63 mm		-	1
	Length: 5–10 mm; Diameter: 0.071–0.315 mm		-	1
Total weight of one specimen, g			730	725

Two asphalt concrete mixtures were designed, following recommendations of GOST 9128-2013. Their recipes are given in Table 1. Both asphalt concrete mixtures were fabricated in the following way:

1. Aggregates were dried out for 12 h at 160 °C.
2. Bitumen was thermostabilized for 2 h at 150 °C.
3. Coarse and fine aggregates were mixed for 10 min at 150 °C.
4. Bitumen was added to mineral fillers and mixed for 30 min at 150 °C.
5. Prepared mixture was kept at 150 °C while samples were being fabricated.

Drier oven Olab Clarity 136 (OmnisLab, Russia) dried out aggregates before mixing. Mixer LS-AB-10 (Novoe Delo, Russia) with temperature control up to 200 °C mixed aggregates with bitumen. Heater PL-HR-capacity (PrimeLab, Russia) kept bitumen at the fixed temperature while samples were being fabricated.

For samples' fabrication, asphalt concrete mixtures were compacted into a cylindrical mold LO-257 (Novoe Delo, Russia) with an inner diameter of d = 71.4 mm, the mold was preheated to 90–100 °C in Olab oven. The asphalt concrete mixture was evenly distributed into molds by bayoneting and then densified within the molds on vibrating platform for 3 min at a frequency of 2900 ± 100 min^{-1}, an amplitude of 0.4 ± 0.05 mm, and a vertical load on mixture 30 ± 0.5 kPa. Then, specimens were compacted with hydraulic press GHP-10 (Gigant, Russia) under pressure 20 ± 0.5 MPa for 3 min. Next, an asphalt concrete specimen was taken out of the mold and cooled down. The final height of specimens was h = 71.4 ± 0.5 mm. For each type of asphalt concrete mixture, 9 specimens were fabricated, three for each mechanical test type.

Asphalt concrete specimens were kept at 25 °C for 5 days before conducting mechanical tests. Three types of mechanical tests were performed for asphalt concrete samples: compressive strength (S_C), compressive modulus (E_C), tension strength (S_T), shear strength (S_S), internal friction coefficient tan(φ), and ultimate percent compression (engineering deformation in compression); ultimate percent compressions at compression test (δ_C), and at indirect tension test (δ_T), were examined and estimated according to GOST 12801.

2.1. Compressive strength test

Initially, specimens were thermostabilized in water for 20 min at 50 °C. After that, a test was conducted with testing machine INSTRON 5969 (Instron, USA) in a vertical position of a specimen (axis of sample's cylindrical symmetry coincides with the loading direction) with the strain rate of 3 mm/min. The loading scheme is presented on Figure 1a.

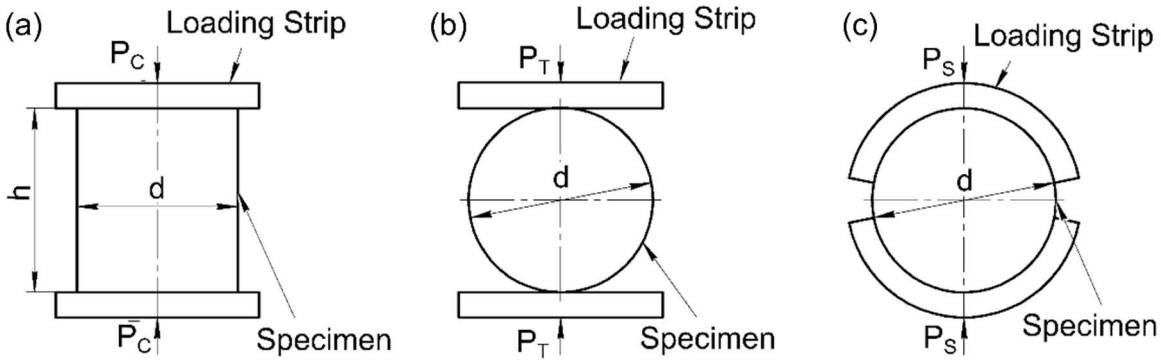

Figure 1. Specimen loading schemes. (a) Compression test, (b) indirect tension test, and (c) shear strength test.

Compressive strength was found with Eq 1:

$$S_C = \frac{P_C^U}{F} \tag{1}$$

where P_C^U is the ultimate applied load required to fail specimen in compression (N), and F is the initial cross-section area of a specimen (m^2).

Compressive modulus was found with Eq 2:

$$E_C = \frac{S_C^b - S_C^a}{\varepsilon_C^b - \varepsilon_C^a} \tag{2}$$

where S_C^a and ε_C^a are compressive strength (N) and strain (mm) at the beginning of the linear part of a stress-strain curve, S_C^b and ε_C^b are at the end of the linear part.

Ultimate percent compression was found with Eq 3:

$$\delta_C = \frac{|h - h_C|}{h} 100\% \tag{3}$$

where h_C is the height of a sample after test (mm).

2.2. Indirect tension strength test

Specimens were thermostabilized in water for 20 min at 0 °C. After that, a test was conducted with testing machine INSTRON 5969 in a horizontal position of a specimen (sample's axis of cylindrical symmetry is perpendicular to loading direction) with the strain rate of 50 mm/min. A loading scheme is shown on Figure 1b.

The tensile strength was determined with Eq 4:

$$S_T = \frac{P_T^U}{hd} \tag{4}$$

where P_T^U is the ultimate applied load required to fail a specimen in indirect tension test (N), h is the height of a specimen (m), and d is the diameter of a specimen (m).

Ultimate percent compression was found with Eq 5:

$$\delta_T = \frac{|d-d_T|}{d}100\% \tag{5}$$

where d_T is the diameter (mm) of a sample after the test. Due to complex stress-strain state in indirect tension test, it is difficult to measure the ultimate percent elongation experimentally. Instead, it may be hypothesized to have a dependence similar to δ_T–both should increase with the increase in ductility and decrease with the increase in brittleness. Therefore, change in δ_T can also serve as an estimation of change in ultimate percent elongation.

2.3. Shear strength test

Specimens also were thermostabilized in water for 20 min at 50 °C. After that, specimens were put into Marshall's breaking head and a test was conducted with testing machine INSTRON 5969 with the strain rate of 50 mm/min. Loading scheme is shown on Figure 1c.

The shear strength was determined with Eq 6:

$$S_S = \frac{1}{6}\big(3 - 2\tan(\phi)\big)S_C^U,\ \tan(\phi) = \frac{3(A_S - A_C)}{3A_S - 2A_C} \tag{6}$$

A_S is the work done on a specimen to deform it in shear strength test (J) and A_C is the work done on a specimen to deform it in compression test (J), as presented by Eq 7:

$$A_S = \frac{P_S\varepsilon_S}{2},\ A_C = \frac{P_C\varepsilon_C}{2} \tag{7}$$

where P_S is the ultimate applied load required to fail a specimen in shear part of the test (N); ε_S is the ultimate strain in shear part of the test (mm), P_C is the ultimate applied load required to fail a specimen in compression part of the test (N), and ε_c is the ultimate strain in compression part of test (mm).

3. Results and discussion

According to the anisotropic structure of road noise-protection fence composite, which is a pultrusion hollow profile, after crushing, the GFRP crumb had a cylindrical shape of different sizes with the length of the crumb being around ten times its diameter, Figure 2a. For the project, only two types of crumb shapes were selected, namely those, whose lengths equal the size of granite crushed

stones, Table 1. Six specimens for shear strength test and three specimens for other tests for each type of asphalt concrete mixture were fabricated. Typical specimens' appearance is shown on Figure 2b.

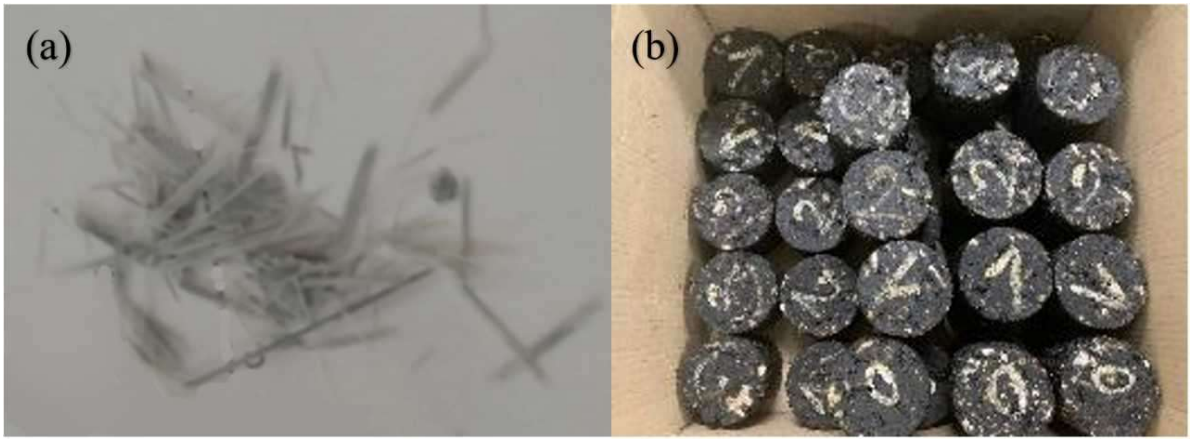

Figure 2. Photo of (a) GFRP crumbs, (b) typical view of asphalt concrete specimens.

From load and deformation data, obtained by mechanical tests, the typical stress-strain curves in compressive and indirect tensile strength tests are plotted on Figure 3. The mechanical characteristics of studied samples were calculated by Eqs 1–7 and are shown in Table 2 (mean ± std) and on Figure 4. A comparative analysis of the influence of the GFRP crumb introduction into the mixture is presented on Figure 5.

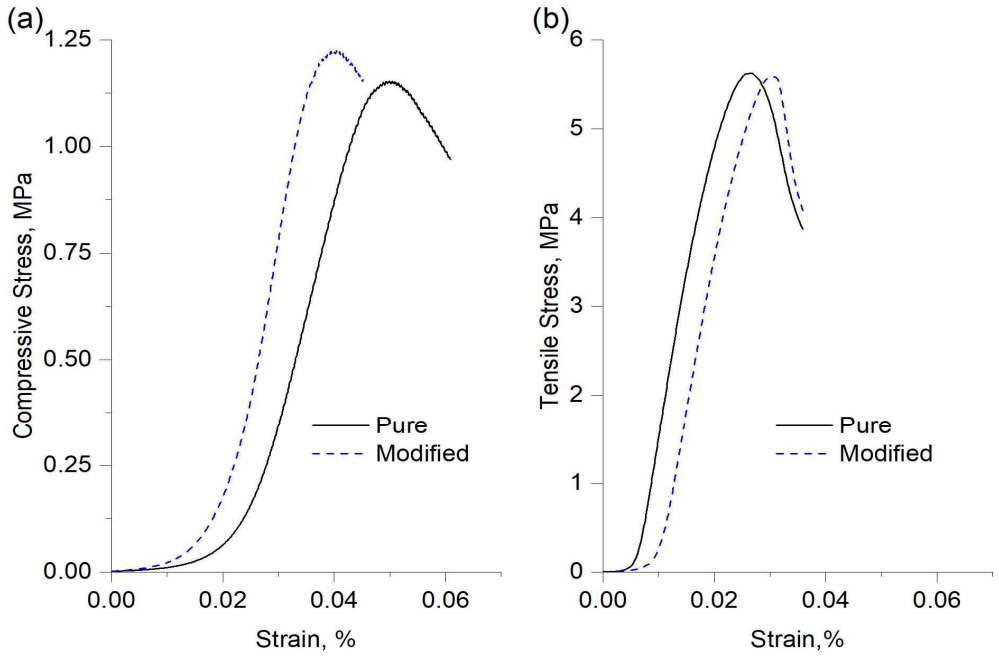

Figure 3. Typical stress-strain curves of asphalt concrete for (a) compressive strength (b) indirect tension strength.

The data in Table 2 show considerable scatter, with coefficient of variation up to 10% for moduli, and up to 25% for strength, which is not surprising given a low number of repetitions (three, as stipulated by the used standards) and variability of the materials.

Table 2. Results of mechanical testing of asphalt concrete.

Type	S_C, MPa	E_C, MPa	S_T, MPa	S_S, MPa	tan(φ)	δ_C, %	δ_T, %
Pure	1.05 ± 0.09	45.4 ± 5.1	5.8 ± 0.55	0.23 ± 0.06	0.85 ± 0.8	2.73 ± 0.07	1.96 ± 0.22
Modified	1.15 ± 0.07	63.8 ± 9.8	5.65 ± 0.06	0.28 ± 0.03	0.75 ± 0.06	2.23 ± 0.21	2.03 ± 0.1

Comparing the curves obtained from the compression test, it is evident that the curve for the modified asphalt concrete has the higher slope than that for the pure asphalt concrete, as shown in Figure 3a. This indicates a higher value of compressive modulus and means that the modified asphalt concrete is more resistant to compression. It is also confirmed by the values of S_c, E_c, and δ_C that were obtained (Table 2 and Figure 4). In the indirect tensile test, the curves for pure and modified asphalt concrete are almost identical, indicating their similar behavior under this type of load, as shown in Figure 3b. Considering account data scatter, differences in values of S_T and δ_T for both types of asphalt concrete can be considered statistically insignificant (Figure 4b). The shear strength test shows that shear strength is improved by GFRP crumb addition while the internal friction coefficient does not change significantly.

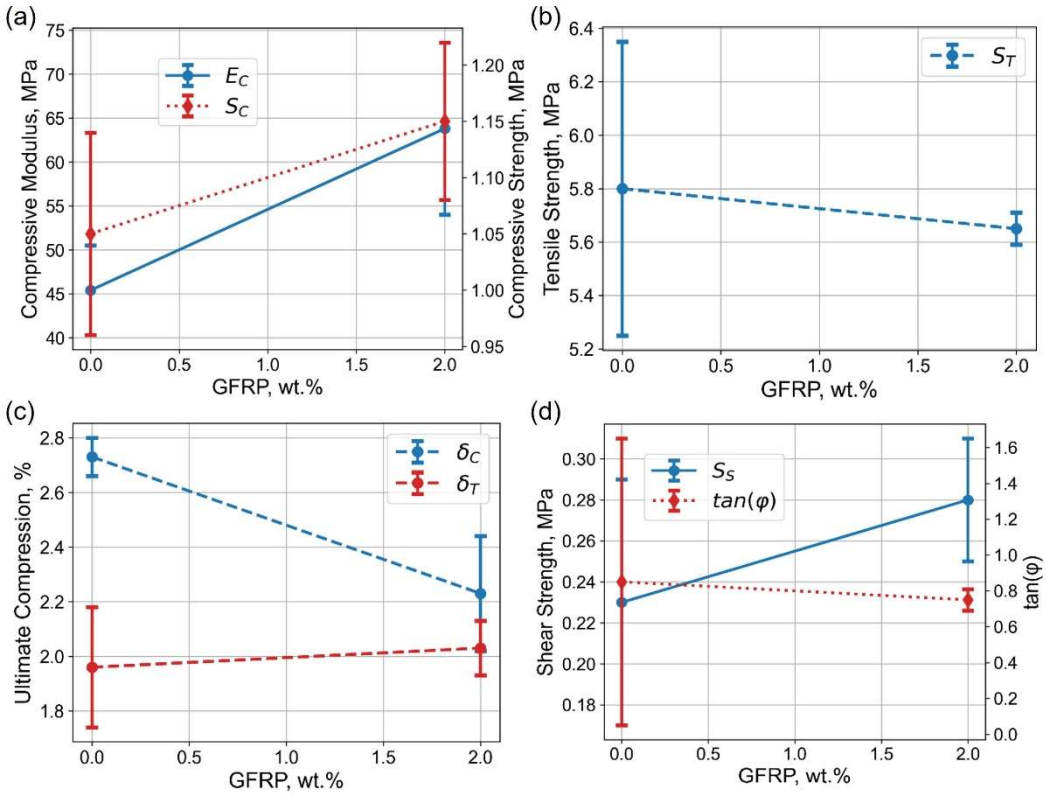

Figure 4. Influence of GFRP crump introduction into asphalt concrete mixture on mechanical properties: (a) compressive modulus and strength, (b) tensile strength, (c) ultimate percent compression, and (d) shear strength and internal friction coefficient.

A comparative analysis of the test results shows a positive influence of GFRP crumb on the properties of asphalt concrete, which can be clearly seen in Figure 5. The greatest increase is observed in the values of compressive modulus indicating a reinforcing effect of the modified asphalt concrete. This may be due to higher aspect ratio of the GFRP crumb, leading to additional binding of aggregates within the asphalt concrete. This is also consistent with the reduction in deformation of the specimens during mechanical testing. In practice, this modification should lead to less rutting formation. It should also be noted that the scatter of properties for modified asphalt concrete samples has a lower value for all conducted studies than for pure asphalt concrete (Table 2 and Figure 4). Therefore, the introduction of GFRP crumb provides a more homogeneous distribution of aggregates within the asphalt concrete mixture.

Only minor deficiencies in mechanical behavior are observed after addition of GFRP crumb. This may signify no adhesion problems between GFRP particles and bitumen. However, these problems may arise, as stated, for example in [17]: the major failure mode in fiber-modified bitumen composites is debonding at the interface between fibers and bitumen, especially for recycled glass. They point to the fact that the recycled glass fibers have a smoother surface than virgin fibers. In the case discussed here, we deal not with fibers, but with GFRP crumbs, which do not have a smooth surface. We can hypothesize that in the studied materials the adhesion between the added GFRP particles and bitumen is sufficient for preventing pre-mature debonding. Apart from a thermosetting polymer in GFRP, the adhesion to bitumen and ways to improve it are also studied for different polymers (see, for example [26–28]). Another factor, which is worth investigating in future work, is moisture effect on different damage modes: the study by Mohammadi et al. [29] shows that increasing content of glass particles increases the resistance of the mixture against wear and moisture damage. The underlying phenomena, defining the increase of the moisture resistance, and possibilities of counteracting the moisture damage using silica nano-particles investigated in detail by Fini et al. [30]. Another approach is to apply aggregate interface coatings [31].

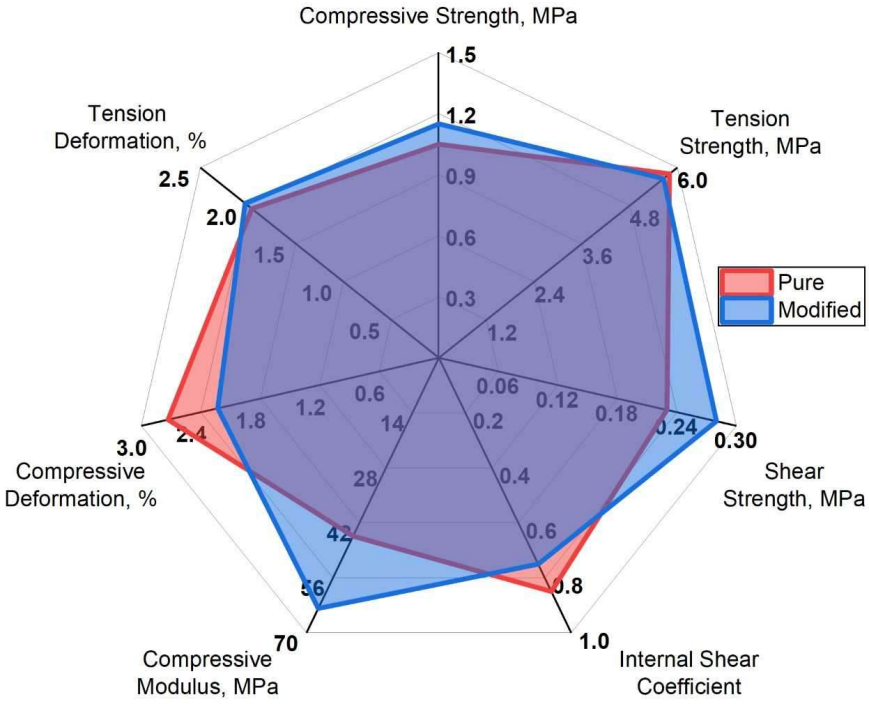

Figure 5. Result of mechanical testing of asphalt concrete.

4. Conclusions

We focused on recycling of glass fiber-reinforced plastics (GFRP) in the production of asphalt concrete by the partial replacement of aggregates with GFRP crumb. The obtained results show that the addition of GFRP crumb to asphalt concrete mixture not only acceptable but improves some of its mechanical properties. The improvement in compressive modulus by 40%, even under conditions of elevated asphalt concrete temperature (tested at 50 °C), demonstrates the relevance of this approach. The top layer of modern road pavement is vulnerable to rutting phenomena, and conducted research can help to solve the problem. Mechanical properties are more significantly improved when the specimen is subjected to axial loading than in the case when subjected to indirect loading. This may be because part of the GFRP crumbs, when forming the specimen, tends to orient vertically due to the bayoneting of the asphalt concrete mixture at samples' fabrication. In the case of volumetric filling, this anisotropic effect in the asphalt concrete will not occur, and indirect tension strength should also increase. Further optimization of the composition of asphalt concrete with GFRP crumb should also lead to an increase in its mechanical properties.

In addition to the mechanical properties, the introduction of GFRP crumbs into asphalt concrete reduces the weight of it approximately by 1%. This is also a positive factor, reducing the load on the soil and saving energy resources during transportation, which are important components of sustainable development.

The main result is the confirmation of the hypothesis that the use of GFRP crumbs in asphalt concrete allows for 100% utilization of GFRP waste, instead of its disposal. This solution is also suitable for the use of GDRP crumb from recycled GFRP waste that was previously buried in landfills. Residual mechanical performance of the GFRP material is utilized at a full-scale compared to other recycling methods. Secondary recycling of GFRP-crumb asphalt concrete is not expected to be influenced by the presence of the GFRP crumbs in it, unless thermosetting nature of crumb resin is unwanted [9]. Also, the necessity to take measures for safety against fiberglass dust at crushing should be mentioned.

Use of AI tools declaration

The authors declare they have not used Artificial Intelligence (AI) tools in the creation of this article.

Acknowledgments

The study was supported by the Russian Science Foundation and city of Moscow, grant 22-23-20170 "Increasing rutting stability and crack resistance of asphalt concrete by utilization of nanostructured polymer and microstructure provided by recycling polymer composite materials with fibrous reinforcement" (https://rscf.ru/project/22-23-20170/).

The authors would like to thank the Mechanical Testing Laboratory, Center for Materials Technologies, Skolkovo Institute of Science and Technology.

Conflict of interest

The authors declare no conflict of interest.

References

1. Morampudi P, Namala KK, Gajjela YK, et al. (2021) Review on glass fiber reinforced polymer composites. *Mater Today Proc* 43: 314–319. https://doi.org/10.1016/j.matpr.2020.11.669
2. Gandia RM, Gomes FC, Corrêa AAR, et al. (2019) Physical, mechanical and thermal behavior of adobe stabilized with glass fiber reinforced polymer waste. *Constr Build Mater* 222: 168–182. https://doi.org/10.1016/j.conbuildmat.2019.06.107
3. Nagrale P (2023) Glass fiber reinforced plastic (GFPR) market research report. Market Research Future. Available at: https://www.marketresearchfuture.com/reports/glass-fiber-reinforced-plastic-gfrp-market-5004.
4. Larsen K (2009) Recycling wind turbine blades. *Renew Energy Focus* 9: 70–73. https://doi.org/10.1016/S1755-0084(09)70045-6
5. Karuppannan Gopalraj S, Kärki T (2020) A review on the recycling of waste carbon fibre/glass fibre-reinforced composites: Fibre recovery, properties and life-cycle analysis. *SN Appl Sci* 2: 433. https://doi.org/10.1007/s42452-020-2195-4
6. Dehghan A, Peterson K, Shvarzman A (2017) Recycled glass fiber reinforced polymer additions to Portland cement concrete. *Constr Build Mater* 146: 238–250. https://doi.org/10.1016/j.conbuildmat.2017.04.011
7. Job S (2013) Recycling glass fibre reinforced composites—history and progress. *Reinf Plast* 57: 19–23. https://doi.org/10.1016/S0034-3617(13)70151-6
8. Liu Y, Farnsworth M, Tiwari A (2017) A review of optimisation techniques used in the composite recycling area: State-of-the-art and steps towards a research agenda. *J Clean Prod* 140: 1775–1781. https://doi.org/10.1016/j.jclepro.2016.08.038
9. Kazemi M, Kabir SF, Fini EH (2021) State of the art in recycling waste thermoplastics and thermosets and their applications in construction. *Resour Conserv Recycl* 174: 105776. https://doi.org/10.1016/j.resconrec.2021.105776
10. Yang Y, Boom R, Irion B, et al. (2012) Recycling of composite materials. *Chem Eng Process* 51: 53–68. https://doi.org/10.1016/j.cep.2011.09.007
11. Torres A (2000) Recycling by pyrolysis of thermoset composites: Characteristics of the liquid and gaseous fuels obtained. *Fuel* 79: 897–902. https://doi.org/10.1016/S0016-2361(99)00220-3
12. Naqvi SR, Prabhakara HM, Bramer EA, et al. (2018) A critical review on recycling of end-of-life carbon fibre/glass fibre reinforced composites waste using pyrolysis towards a circular economy. *Resour Conserv Recycl* 136: 118–129. https://doi.org/10.1016/j.resconrec.2018.04.013
13. Gharde S, Kandasubramanian B (2019) Mechanothermal and chemical recycling methodologies for the fibre reinforced plastic (FRP). *Environ Technol Inno* 14: 100311. https://doi.org/10.1016/j.eti.2019.01.005
14. Mattsson C, André A, Juntikka M, et al. (2020) Chemical recycling of end-of-life wind turbine blades by solvolysis/HTL. *IOP Conf Ser Mater Sci Eng* 942: 012013. https://doi.org/10.1088/1757-899X/942/1/012013

15. Gonçalves RM, Martinho A, Oliveira JP (2022) Recycling of reinforced glass fibers waste: Current status. *Materials* 15: 1596. https://doi.org/10.3390/ma15041596
16. Tao Y, Hadigheh SA, Wei Y (2023) Recycling of glass fibre reinforced polymer (GFRP) composite wastes in concrete: A critical review and cost benefit analysis. *Structures* 53: 1540–1556. https://doi.org/10.1016/j.istruc.2023.05.018
17. Yang Q, Fan Z, Yang X, et al. (2023) Recycling waste fiber-reinforced polymer composites for low-carbon asphalt concrete: The effects of recycled glass fibers on the durability of bituminous composites. *J Clean Prod* 423: 138692. https://doi.org/10.1016/j.jclepro.2023.138692
18. Thamizh Selvan R, Vishakh Raja P, Mangal P, et al. (2021) Recycling technology of epoxy glass fiber and epoxy carbon fiber composites used in aerospace vehicles. *J Compos Mater* 55: 3281–3292. https://doi.org/10.1177/00219983211011532
19. Li YF, Hsu YW, Syu JY, et al. (2023) Study on the utilization of waste thermoset glass fiber-reinforced polymer in normal strength concrete and controlled low strength material. *Materials* 16: 3552. https://doi.org/10.3390/ma16093552
20. Krzywiński K, Sadowski Ł, Piechówka-Mielnik M (2021) Engineering of composite materials made of epoxy resins modified with recycled fine aggregate. *Sci Eng Compos Mater* 28: 276–284. https://doi.org/10.1515/secm-2021-0029
21. Yang Q, Fan Z, Yang X, et al. (2023) Recycling waste fiber-reinforced polymer composites for low-carbon asphalt concrete: The effects of recycled glass fibers on the durability of bituminous composites. *J Clean Prod* 423: 138692. https://doi.org/10.1016/j.jclepro.2023.138692
22. Hogan DJ, Morrison M, Desai A (2020) Fiberglass, dusts, In: John S, Johansen J, Rustemeyer T, et al. *Kanerva's Occupational Dermatology*, Switzerland: Springer Cham. https://doi.org/10.1007/978-3-319-68617-2_38
23. Wache S, Helmig S, Walter D, et al. (2017) Impact of biopersistent fibrous dusts on glycolysis, glutaminolysis and serine metabolism in A549 cells. *Mol Med Rep* 16: 9233–9241. https://doi.org/10.3892/mmr.2017.7729
24. Du ZF, Zhang S, Zhou QJ, et al. (2018) Hazardous materials analysis and disposal procedures during ship recycling. *Resour Conserv Recycl* 131: 158–171. https://doi.org/10.1016/j.resconrec.2018.01.006
25. Sattler T, Pomberger R, Schimek J, et al. (2020) Mineral wool waste in Austria, associated health aspects and recycling options. *Detritus* 9: 174–180. https://doi.org/10.31025/2611-4135/2020.13904
26. Faisal Kabir S, Sukumaran S, Moghtadernejad S, et al. (2021) End of life plastics to enhance sustainability of pavement construction utilizing a hybrid treatment of bio-oil and carbon coating. *Constr Build Mater* 278: 122444. https://doi.org/10.1016/j.conbuildmat.2021.122444
27. Aldagari S, Kabir SF, Lamanna A, et al. (2022) Functionalized waste plastic granules to enhance sustainability of bituminous composites. *Resour Conserv Recycl* 183: 106353. https://doi.org/10.1016/j.resconrec.2022.106353
28. Shariati S, Aldagari S, Fini EH (2023) Bio-modifier: A sustainable suturing technology at the bitumen–aggregate interface. *ACS Sustainable Chem Eng* 11: 8908–8915. https://doi.org/10.1021/acssuschemeng.3c01001
29. Mohammadi MM, Asadi Azadgoleh M, Ghodrati A, et al. (2023) Introducing waste glass powder as a sustainable constituent in microsurfacing. *Constr Build Mater* 395: 132271. https://doi.org/10.1016/j.conbuildmat.2023.132271

30. Fini EH, Hung AM, Roy A (2019) Active mineral fillers arrest migrations of alkane acids to the interface of bitumen and siliceous surfaces. *ACS Sustainable Chem Eng* 7: 10340–10348. https://doi.org/10.1021/acssuschemeng.9b00352
31. Aldagari S, Hung AM, Shariati S, et al. (2022) Enhanced sustainability at the bitumen-aggregate interface using organosilane coating technology. *Constr Build Mater* 359: 129500. https://doi.org/10.1016/j.conbuildmat.2022.129500

AIMS Press